

## Wall effects on a sphere translating at constant velocity

By A. AMBARI†, B. GAUTHIER-MANUEL AND E. GUYON

Laboratoire d'Hydrodynamique et de Mécanique Physique, ERA N° 1000, ESPCI,  
10 rue Vauquelin, 75231 Paris Cedex 05

(Received 12 April 1984)

We present experimental results on the modified Stokes force  $F$  exerted on a sphere in magnetic levitation whose position is kept fixed by an optical feedback system. A Newtonian liquid moves at a constant velocity  $U$  relative to the sphere. We consider the motion in two different situations.

(i) When the sphere approaches a wall perpendicular to  $U$ , the increase in  $|F|$  due to lubrication agrees quantitatively with theoretical results such as those of Brenner (1961) and Maude (1961), obtained neglecting the unsteadiness of the flow field.

(ii) In the complementary situation of a sphere moving along the axis of a cylindrical tube, our results expressed as a function of the eccentricity of the trajectory and of the ratio of the two radii confirm and extend previous theoretical analyses. They show in particular the existence of a minimum of  $|F|$  away from the axis of the cylinder and a sharp increase in  $|F|$  when the sphere approaches the sidewall. By comparing with the results for a sphere moving parallel to a flat wall, we analyse the effect of the curvature of the cylindrical tube.

---

### 1. Introduction

A logical first step towards the elucidation of the hydrodynamic behaviour of suspensions of spherical particles is the study of the hydrodynamic interactions between individual particles, of particle motion in the presence of bounding walls and of combinations of these two events. The interactions are caused by the long-range velocity distribution generated in the fluid surrounding each moving particle; they control the distribution of the particles. In turn, the distribution itself determines the dynamical behaviour of each individual particle.

For instance, in sedimentation the average speed of fall of a particle depends on concentration; the dependence, mainly due to the hydrodynamic interactions, was studied theoretically by Batchelor (1972).

A major difficulty in the experimental determination of these interactions comes from the absence of control of the spatial location of each particle within the bed of particles or near fixed walls, as the particles move under an external force field or in an imposed velocity field.

In this paper we describe an original method for the measurement of the hydrodynamic force impressed on an individual sphere when the law of displacement is imposed externally.

The technique had been introduced in our laboratory as a rheometric method to study the viscosity and elasticity during a gelation process (Gauthier-Manuel & Guyon

† Also Laboratoire de Physique des Liquides et Electrochimie, Université P. et M. Curie, T 22, 4 place Jussieu, 75230 Paris Cedex 05.

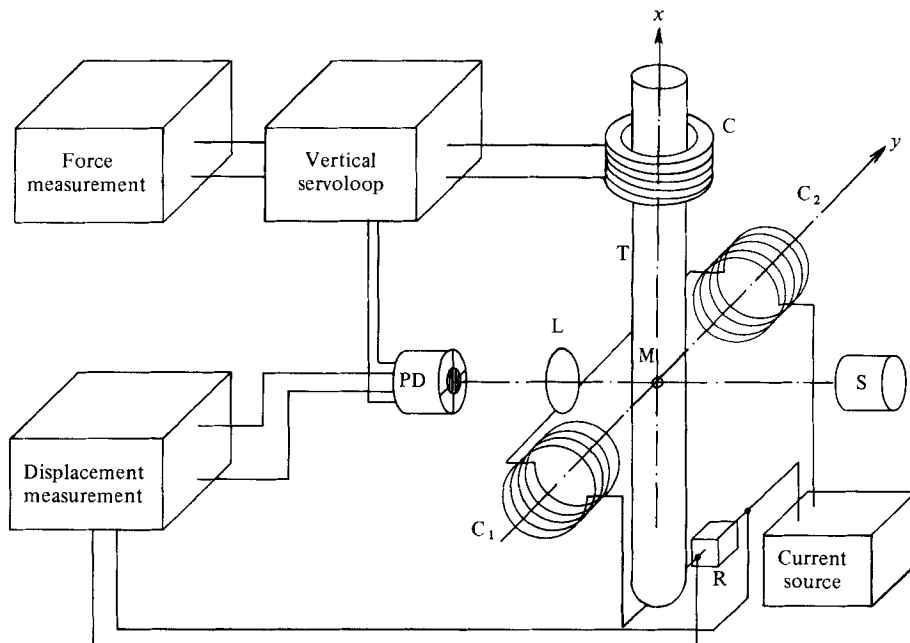


FIGURE 1. Experimental apparatus: M, magnetic sphere; C, levitation coil; ( $C_1$ ,  $C_2$ ), deviation coils; PD, four-quadrant photodiodes; S, lamp source; L, microscope objective; T, tube.

1980); a technical description of the sphere rheometer is given in Gauthier-Manuel, Meyer & Pieranski (1984). It was first used by Ambari, Gauthier-Manuel & Guyon (1983) in the context of the present project to study the effect of a plane wall on the hydrodynamic force exerted on a sphere moving parallel to it at a constant velocity. The results were compared with the theoretical models of O'Neill (1964), O'Neill & Stewartson (1967), Goldman, Cox & Brenner (1967) and Faxén (1921). The results are summarized in §4 of this paper.

In §3 we present experimental results on the hydrodynamic force exerted on a sphere moving towards a plane wall at a fixed velocity. The method leads to a continuous measurement of the variation of the force. This study was made at different low Reynolds numbers  $Re \sim 10^{-4}$ . The results are compared with the theoretical calculations of Maude (1961) and Brenner (1961). The present study deals with hydrodynamic wall effects at small separations, but could easily be extended to a sphere approaching a surface of spherical or cylindrical shape. Such wall effects play an essential role in the dynamical behaviour of non-dilute suspensions, as stressed in particular by de Gennes (1981) in the study of plug flow of such suspensions. It is also of direct importance in problems of aggregation of particles or in their capture (filtration).

In §4 we present some original experimental results on the variation of the hydrodynamic force exerted on an eccentrically positioned sphere in a circular cylindrical tube filled with a Newtonian fluid. The displacement of the sphere takes place without rotation in the axial direction; the force is measured as a function of the eccentricity and of the reduced diameter of the sphere. The study provides a direct verification of the theoretical predictions of Brenner & Happel (1958). As far as we know, there is no other direct quantitative experimental data in the literature concerning this problem. A striking result obtained is that the drag force decreases

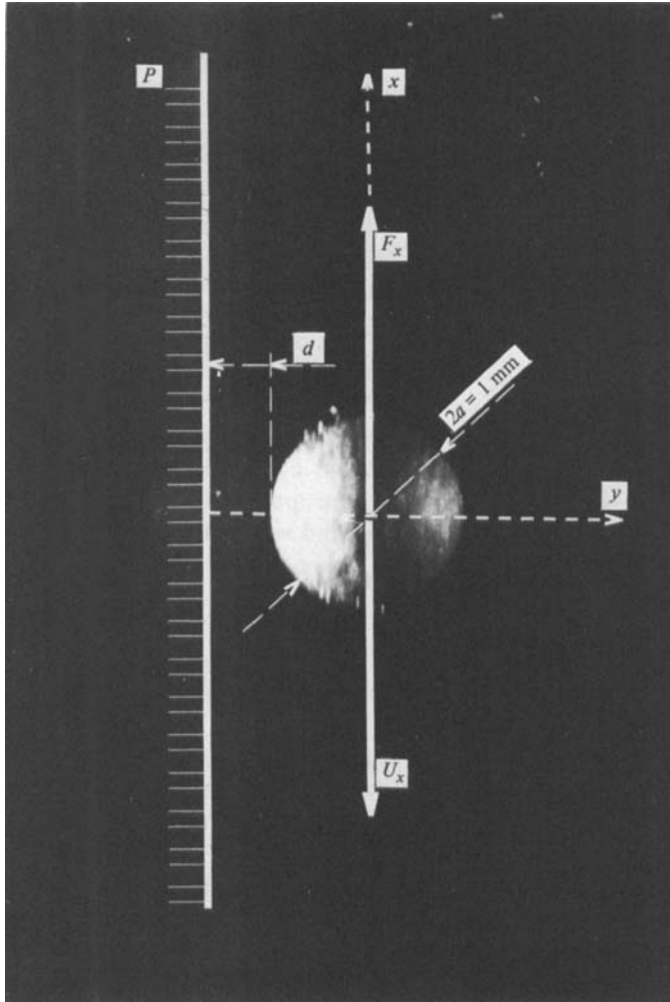


FIGURE 2. Photograph of a sphere of diameter  $2a = 1.0$  mm near a vertical plane  $P$ .

and goes through a minimum as the sphere moves away from the tube axis. The results are also compared with the theoretical calculations of Tözeren (1983) for small eccentricities in a more limited range of parameters. Applications of this last study are numerous, and range from falling-ball viscosimeters, capillary blood flow to flow of particles in porous materials, which are often visualized as a bundle of tubes.

## 2. Experimental

### 2.1. The sphere rheometer

The sphere rheometer was initially built to study the viscous and elastic behaviour during the formation of transparent gels. A first application to the study of the viscous behaviour of spheres in limited geometries was described in Ambari *et al.* (1983), and a detailed description of the experimental set-up can be found in Gauthier-Manuel *et al.* (1984). We will only recall its essential elements.

Figure 1 is a schematic view of the apparatus. It uses a magnetic sphere maintained

in a fixed position by magnetic levitation (figure 2) within a mobile experimental cell containing a Newtonian fluid of viscosity  $\eta$  (Rhodorsil silicone oil). The vertical stability of the sphere (M) is obtained using a feedback loop. A microscope objective (L) forms the image of the sphere, lit by a 15 W lamp source (S), on a differential photodiode (PD). The difference of the area of the shadow of M between the quadrants of the upper and lower halves of the photodiode when the sphere moves vertically from its central position is amplified into a control current, which is sent into a levitating coil (C), which provides a vertical magnetic induction  $B_x$ . The vertical force on the sphere of magnetization  $\mu$  is

$$F_{mx} = \mu \cdot \nabla B_x.$$

The induction field  $\mathbf{B}$  also ensures horizontal radial equilibrium of the sphere.

In static conditions the magnetic force  $F_{mx}$  exactly balances the apparent weight of the sphere (corrected by buoyancy). When the cell (tube T on figure 1) moves at a constant vertical velocity  $U_x$ , a hydrodynamic friction force  $F_x$  adds to or subtracts from the apparent weight, depending on the sign of  $U_x$ . The control current varies to keep the sphere fixed. This variation is proportional to the hydrodynamic force, which, for a cell of dimensions large compared with that of the sphere, is the Stokes result:

$$F_s = 6\pi\eta a U_x, \quad (2.1)$$

where  $a$  is the radius of the sphere.

The electronic time constant ( $\sim 10^{-2}$  s) (see Gauthier-Manuel *et al.* 1984) is always shorter than the convective timescale  $a/U_x$  ( $\sim 10$  s). In non-stationary cases, like the near approach of a sphere to a wall, the spacing of the data points (as given on figure 5) is limited by that of the acquisition chain (20 ms), and there is no reason to expect an appreciable effect of the electronic response for such data.

The control current is recorded continuously using a programmable multichannel analyser (Tracor) with an accuracy of 1%.

The horizontal position of the sphere can be controlled using a pair of Helmholtz coils ( $C_1$ ,  $C_2$ ) of horizontal axis mounted in opposition, which provides a constant gradient of induction near the centre  $O$  of the cell. The constant horizontal force  $F_{my}$  opposes the restoring horizontal force due to the field in the coil (C). The equilibrium distance  $c$  from the centre of the sphere to  $O$  is an increasing function of the current in the coils ( $C_1$ ,  $C_2$ ).

## 2.2. Calibration

The photodiode system (PD) has four quadrants and can also be used to determine the difference in intensity of light due to a horizontal displacement of the shadow of the sphere. We have checked that the detection of the horizontal displacement  $c$  of the sphere is linear to better than 0.7% for a value of  $c$  lower or equal to 40% of its radius ( $c = 0.17$  mm for a sphere of diameter 0.87 mm). The sensitivity of the detection of 1 mV per  $\mu\text{m}$  is large, and suitable for very small displacements. For larger displacements, we use the direct measurement of the voltage  $V_B$  applied to the coils ( $C_1$ ,  $C_2$ ). Figure 3 gives  $V_B$  as a function of the reduced distance  $e = c/R$  measured from photographs. In experimental conditions (radius  $a = 0.6$  mm, radius of the tube T  $R = 5$  mm), a good linearity is obtained up to a value of  $c = 4.4$  mm corresponding to the contact of the sphere with the tube.

The vertical displacement of the cell is known with an accuracy of 1  $\mu\text{m}$  using a displacement gauge attached to it. Absolute displacements have also been obtained from photographs, using the accurately known sphere radius for calibration.

The temperature of the cell is regulated to  $25 \pm 0.1$  °C by circulating water from

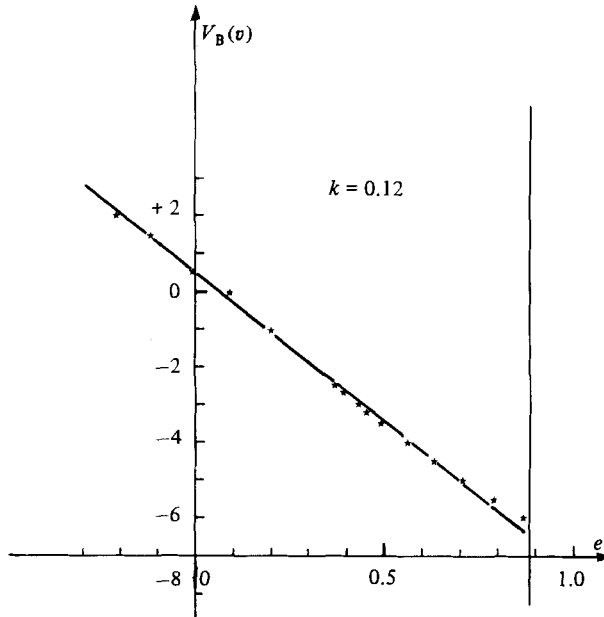


FIGURE 3. Measurement of the voltage  $V_B$  applied to the coils ( $C_1$ ,  $C_2$ ) plotted as a function of the reduced distance to the axis  $e = c/R$ , measured from photographs (for  $R = 5$  mm and  $k = a/R = 0.12$ ).

a thermostatic bath in a jacket surrounding the cell to avoid thermal-convection effects which could be induced in the cell by the lamp source. The heat dissipated by induction in the sphere is also totally negligible with the horizontal and vertical fields used ( $\sim 10^{-3}$  and  $10^{-5}$  T). We may note, however, that (as suggested by a referee) the study of the variation of the Stokes force for larger heating current could provide original information on the convection currents within such a cell. At this temperature, the kinematic viscosity of the Rhodorsil silicone oil used (47 V 100) is  $\nu = 10^{-4} \text{ m}^2 \text{ s}^{-1}$ .

### 2.3. Rotation of the sphere

The sphere is equivalent to a magnetic moment  $\mu$  attached to the sphere which aligns along the induction field  $\mathbf{B}$  under the influence of a magnetic torque  $\mathbf{\Gamma}_m = \mu \times \mathbf{B}$ . In most experimental situations, a hydrodynamic torque  $\Gamma_z$  accompanies the hydrodynamic Stokes force  $F_x$ . As we only want to study the linear relation between the velocity  $U_x$  and the force without influence of the rotation of the sphere we must make sure that no appreciable rotation is obtained.

Using an estimate of  $\Gamma_z \approx 2 \times 10^{-8} \text{ N m}$  and the results of the theoretical calculation given in §4.2, we find an equilibrium angle of rotation given by  $\sin \theta = \Gamma_z / \mu B$ . For  $\mu \approx 10^{-3} \text{ J T}^{-1}$ ,  $B = 2 \times 10^{-3} \text{ T}$ . The rotation angle  $\theta \approx 10^{-2} \text{ rad}$  is very small, and no permanent rotational motion should take place.

## 3. Effect of a plane wall on a sphere moving perpendicular to it

In this section we consider the effect of a plane wall on the hydrodynamic force exerted on a sphere moving towards it. We record continuously the increase of the force when the sphere moves towards the plane with a constant speed at a low Reynolds number.

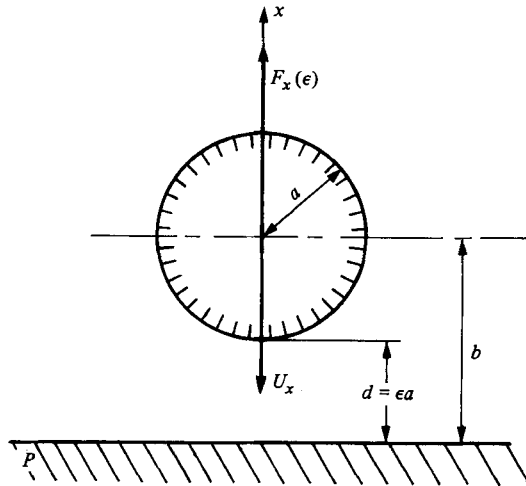


FIGURE 4. Sketch of the geometry of the experiment dealing with a sphere approaching a horizontal plane *P*.

3.1. *Formulation of the problem*

Figure 4 gives the geometry of the experiment. The sphere moves at a fixed velocity  $U_x$  towards the rigid plane ( $x = 0$ ), the upper half-space ( $x > 0$ ) being filled with a Newtonian fluid of known viscosity  $\eta$  (this description is given in a reference frame moving at a velocity  $-U_x$  with the plane which is the bottom wall of the cell; in an absolute reference frame, the sphere is fixed). The problem is geometrically unsteady due to the linear variation of the distance  $d$  (and of  $b = d + a$ ) with time. We defer the discussion to the end of the paragraph and assume first that a quasi-static solution applies ( $DV/Dt = 0$ ). A correction factor  $\delta(\epsilon)$  (where  $\epsilon = d/a$ ) in the Stokes force has been obtained independently by Maude (1961) and Brenner (1961) using bipolar coordinates which had been used first by Stimson & Jeffrey (1926):

$$F_x(\epsilon) = 6\pi\eta a U_x \delta(\epsilon) \tag{3.1}$$

$$\delta(\epsilon) = \frac{4}{3} \sinh \alpha \sum_{n=1}^{\infty} \frac{n(n+1)}{(2n-1)(2n+3)} \left[ \frac{2 \sinh(2n+1)\alpha + (2n+1) \sinh 2\alpha}{4 \sinh^2(n+\frac{1}{2})\alpha - (2n+1)^2 \sinh^2 \alpha} - 1 \right], \tag{3.2}$$

where

$$\alpha = \cosh^{-1}(1 + \epsilon).$$

The expression (3.2) reduces to the result obtained by Lorentz (1907) for large separations ( $\epsilon \gg 1$ )

$$\delta(\epsilon) \simeq 1 + \frac{9}{8} \frac{1}{1 + \epsilon}, \tag{3.3}$$

and to that attributed to Taylor in the lubrication limit  $\epsilon \rightarrow 0$

$$\delta(\epsilon) \simeq \epsilon^{-1}, \tag{3.4}$$

which can be derived from the asymptotic expansion of (3.2) given by Cox & Brenner (1967)

$$\delta(\epsilon) \underset{\epsilon \rightarrow 0}{\simeq} \epsilon^{-1} \left( 1 - \frac{1}{5}\epsilon \ln \epsilon + 0.9712\epsilon \right). \tag{3.5}$$

Let us consider more closely the condition of validity of quasi-static flows. The

problem is geometrically unsteady owing to the variation of the distance  $d$ . In the Navier–Stokes equation a term  $\partial v/\partial t$  must be added to the convective acceleration  $(\mathbf{v} \cdot \nabla) \mathbf{v}$ . The existence of the two terms implies that the direction of motion of the sphere with respect to the plane does not just change the sign of the force as it would do in a time-reversible Stokes solution.

The condition of quasi-static flow was expressed by Cox & Brenner (1967) in the form  $\epsilon Re \ll 1$ . The condition can be found by expressing that the velocity field in the gap created by the relative motion of the sphere with respect to the wall must establish itself by viscous diffusion in a time characteristic of the non-stationary flow  $d/U_x$ . Taking the distance as  $d$  we get the condition

$$d^2/\nu \ll d/U_x$$

or

$$Re (= U_x a/\nu) \ll \epsilon^{-1}. \quad (3.6)$$

On the other hand, in the lubrication limit ( $\epsilon \ll 1$ ), the geometrical distance for the establishment of the velocity field around the whole sphere is of the order of the radius of the sphere  $a$  (instead of  $d$ ); this gives another condition in this limit

$$a^2/\nu \ll d/U_x$$

or

$$Re \ll \epsilon. \quad (3.7)$$

This relation (3.7) is also given by Cooley & O'Neill (1969).

In conclusion, we expect that inertial terms due to convective and local accelerations caused by the changing geometry can be neglected if both relations (3.6) and (3.7) are satisfied. We will see that the conditions are fulfilled in the present experiments. The use of, say, larger objects moving at the same velocity would permit a study of such non-stationary terms.

### 3.2. Method and experimental results

We have used the set-up described in §2. The cylindrical tube has a flat horizontal bottom and moves at a constant velocity  $-U_x$  while the sphere is kept fixed along the central axis of the cell. The cell is filled with silicone oil up to a level much higher than that of the sphere to make free-surface effects negligible. The position  $d = \epsilon a$  of the sphere with respect to the plane is obtained, *a posteriori*, from the known velocity of the tube and from the instant of ‘contact’ between the sphere and the plane at which the force diverges; this time can be deduced from an extrapolation of the force increase using the asymptotic relation (3.4). Thus  $d$  is determined with an accuracy  $U_x \Delta t$  where  $\Delta t = 0.02$  s is the time unit of data acquisition of the multichannel analyser used in the experiment.

Far from the plane, the Stokes hydrodynamic force must be corrected for the effect of the lateral walls of the cylindrical cell of radius  $R$  ( $2a = 0.87$  mm and  $2R = 10$  mm in the experiment):

$$F_x(\infty) = \lambda_0 \frac{(a)}{R} F_S, \quad (3.8)$$

where  $F_S$  is the bulk Stokes force (2.1). Near the plane, (3.1) must be replaced, using (3.8), by

$$F_x(\epsilon) = \delta(\epsilon) F_x(\infty).$$

On figures 5(*a*, *b*) we have plotted the theoretical variation of  $\delta(\epsilon)$  calculated from the exact expression (3.2). On the same figures, we also show our experimental results, corresponding to values of  $\epsilon$  in the range  $1.9 \times 10^{-2} < \epsilon < 1.15$  and to a velocity

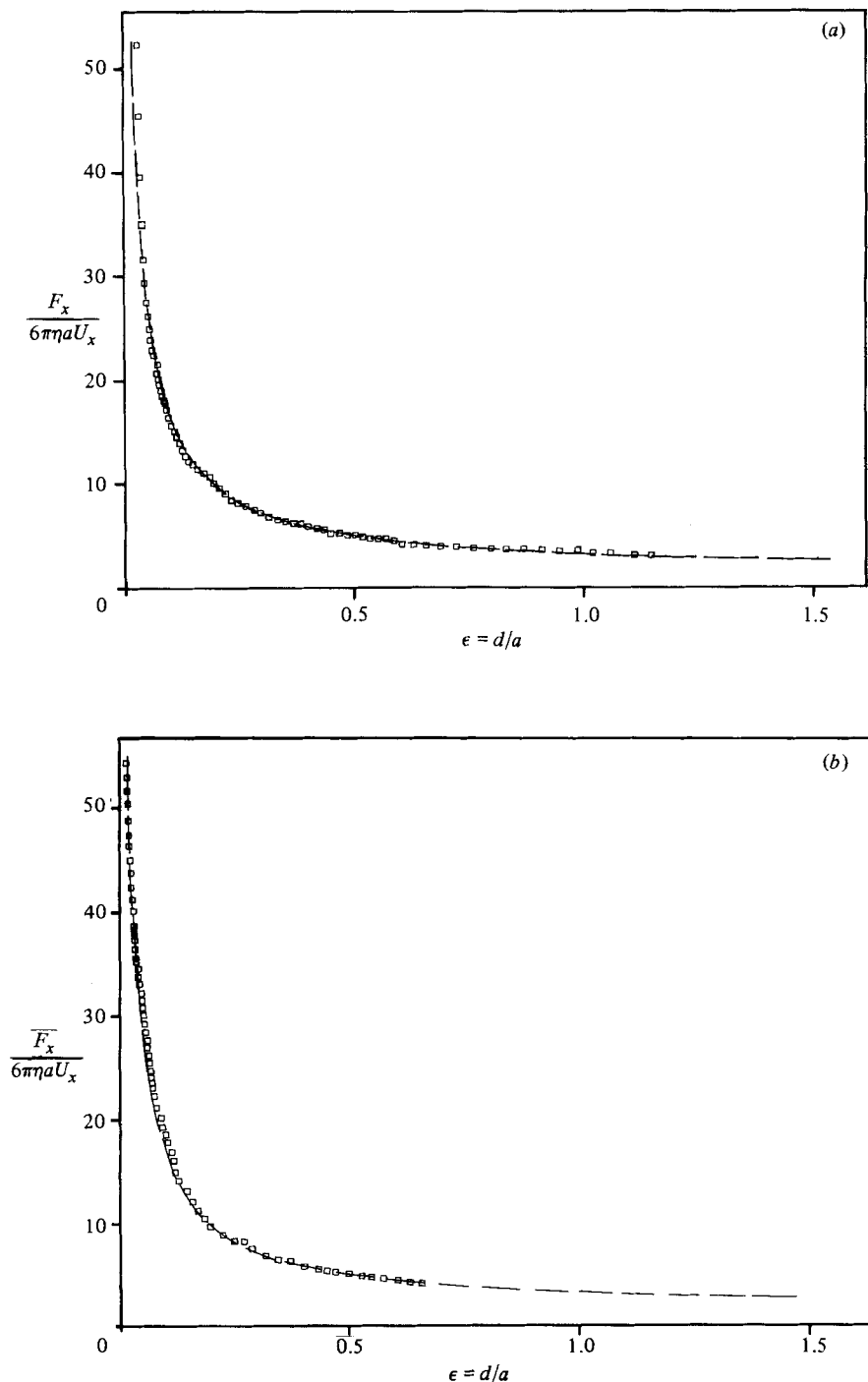


FIGURE 5. The drag force on the sphere normalized to the Stokes value  $F_x(\epsilon)/(6\pi\eta a U_x)$  is plotted versus the reduced distance to the horizontal wall  $\epsilon = d/a$ . The curve shows the increase of the force due to lubrication as the sphere approaches the wall. —, theoretical curve (a)  $\square$ , experimental values for  $Re = U_x a/\nu \sim 2.9 \times 10^{-4}$ ,  $\nu = 10^{-4} \text{ m}^2 \text{ s}^{-1}$  (silicone oil 47V100),  $U_x = 6.7 \times 10^{-5} \text{ m s}^{-1}$ ,  $a = 0.435 \text{ mm}$ . (b)  $\square$ , experimental values for  $Re = 1.45 \times 10^{-4}$ ,  $\nu = 10^{-4} \text{ m}^2 \text{ s}^{-1}$ ;  $U_x = 3.5 \times 10^{-5} \text{ m s}^{-1}$ ;  $a = 0.435 \text{ mm}$ .



$U_x = 6.7 \times 10^{-5} \text{ m s}^{-1}$  for figure 5(a) to the values of  $1.8 \times 10^{-2} < \epsilon < 0.66$  and to a velocity  $U_x = 3.3 \times 10^{-5} \text{ m s}^{-1}$  for figure 5(b).

The Reynolds numbers  $Re = U_x a / \nu$  respectively equal to  $2.9 \times 10^{-4}$  and  $1.45 \times 10^{-4}$  are sufficiently small and allow satisfaction of the two relations (3.6) and (3.7); thus the quasi-static approximation is justified. The smallest value of  $\epsilon$  corresponds to  $d_{\min} = 8 \mu\text{m}$  and to a value of the ratio  $\delta(\epsilon) = 54$  times that taken at infinity; it still fulfils condition (3.7).

We also note that the London–Van der Waals attractive forces are completely negligible at these large distances, compared with the hydrodynamic ones.

The agreement between theory and experiment is excellent, as can be seen on figures 5(a, b). It was verified for a number of experiments with variable but small  $Re$  obtained by varying  $U_x$  or  $\nu$ . The results can be compared with those obtained by Mackay & Mason (1961), Mackay, Suzuki & Mason (1961) and Yuu & Fukui (1981). A major difference between these results and the present ones is the fact that we impose well-defined hydrodynamic conditions (in particular,  $Re$  is constant in the experiment up to the contact) whereas the previous works with an imposed external force  $= \frac{4}{3}\pi a^3(\rho_s - \rho)g$  (apparent weight of the sphere of density  $\rho_s$ ) have a continuously variable Reynolds number from  $Re_\infty$  far from plane to  $Re = 0$  at the contact. However, when  $Re_\infty$  is small and  $\frac{2}{9}(a^3/\nu^2)(\rho_s - \rho)g/\rho \ll 1$  as given by Cooley & O'Neill (1969) we find similar results with both types of studies.

We intend to broaden the comparison beyond the quasi-static approximation by using magnetic particles embedded in spheres with a larger radius  $a$ . The inertial effects met in the present problem and resulting from the presence of both convective and local acceleration terms in the complete Navier–Stokes equations must be studied at a fixed Reynolds number as the sphere approaches the plane. This condition can only be realized by the present experiment. If the force is imposed, the Reynolds number decreases to zero when the sphere approaches the wall because the force  $F_x$  goes to infinity in the lubrication limit.

#### 4. Off-axis motion of a sphere in a fluid-filled cylindrical tube

In this study, we consider the variation of the hydrodynamic force exerted on a sphere positioned eccentrically within a cylindrical tube filled with Newtonian fluid and translating along the axial direction without rotation.

##### 4.1. Formulation of the problem and experimental results

The parameters of the experiment are given on figure 6. The study is made as a function of the two dimensionless variables: the reduced radius  $k = a/R$  of the sphere and the eccentricity  $e = c/R$  of the sphere trajectory.

The eccentricity ratio  $e$  varies from 0 along the cylinder axis to  $e_{\max} = 1 - k$  as the sphere touches the sidewalls. The position is controlled by the current sent into the pair of coils ( $C_1, C_2$ ) as described in §2.2. The tube is displaced vertically at a constant velocity  $U_x = 6.7 \times 10^{-4} \text{ m s}^{-1}$  in all the experiments. The velocity is small enough so that the flow takes place in the Stokes regime ( $Re \sim 10^{-3}$ ).

In figures 8(a–e) we give the experimental results of the force  $F_x(e, k)$ , normalized to its value measured on the axis,  $F_x(0, k)$ , for two spheres ( $2a = 1 \text{ mm}$  and  $2a = 0.87 \text{ mm}$ ) as a function of  $e$ , for different reduced radii  $k = 0.12$  (8a), 0.17 (8b), 0.29 (8c), 0.44 (8d), 0.6 (8e).

The experimental set-up has already been described in §2. It uses a magnetic sphere

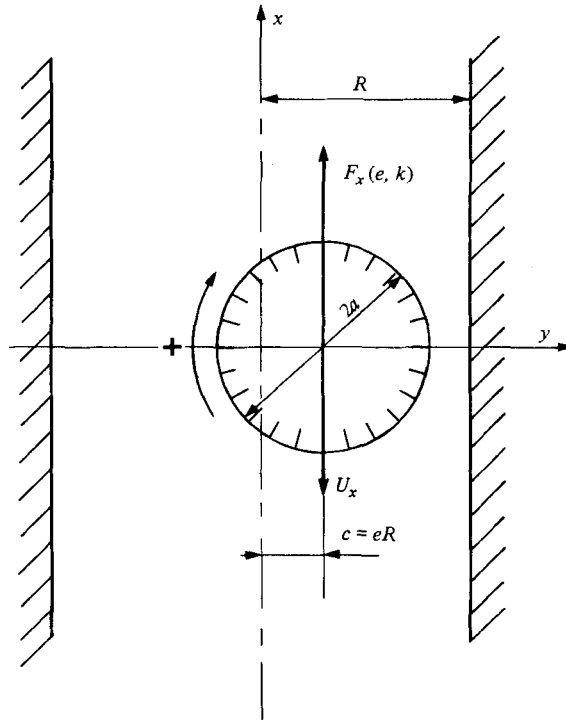


FIGURE 6. Sketch of the experimental geometry for the off-axis motion of a sphere along a fluid-filled cylindrical tube of radius  $R$ .

of radius  $a$  kept in a fixed position in vertical glass tubes of different diameters  $2R$  (10, 5, 3, 2 and 1.45 mm) filled with silicone oil.

#### 4.2. Comparison with theory

This study provides a direct check on various theoretical models which have not yet received a direct experimental assessment. It also goes beyond the range of application of these analyses. In fact, a theoretical analysis of this problem showing a decrease of the force away from the axis, which we observe experimentally, had been made long ago by Brenner & Happel (1958, 1973). Their calculation, using the method of 'reflections' which is valid for  $k \ll 1$ , led to the following expression:

$$F_x(e, k) = 6\pi\eta a U_x [1 + kf(e) + \dots], \quad (4.1)$$

with

$$f(e) = 2.10444 - 0.6977e^2 + O(e^4). \quad (4.2)$$

This expansion is valid for eccentricities  $e \rightarrow 0$  (near the cylinder axis). The function  $f(e)$  has been calculated as a power series in  $e$ , and tabulated by Happel & Brenner (1973) and Famularo (1962). Their results indicate that the drag experienced by a small sphere translating at a fixed velocity in a quiescent fluid does not increase monotonically as we proceed outward from the cylinder axis towards the wall. Rather, it attains a minimum value at  $e \approx 0.4$ . At a larger distance from the wall ( $e \approx 0.55$ ), it recovers the value it has on the axis of the tube. Similar results are obtained in the present experiment for a large range of values of the reduced radii  $k$ .

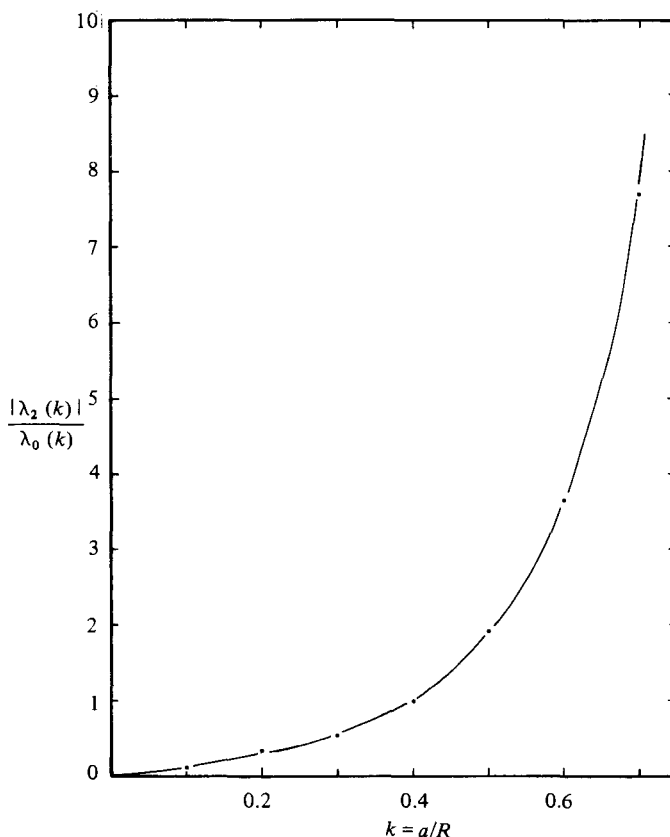


FIGURE 7. The function  $|\lambda_2(k)|/\lambda_0(k)$  calculated from Tözeren's results ( $\lambda_0(k)$  is given in table 1 and  $\lambda_2(k)$  in table 4 of Tözeren (1983) is plotted versus the reduced radius  $k = a/R$ .

On the other hand, the frictional torque  $\Gamma_z$  (about the sphere centre) experienced by the sphere is an odd function of  $e$ . This is physically obvious since the sphere will tend to rotate in a direction opposite to its original direction and at the same angular velocity when it is placed symmetrically with respect to the cylinder axis. The torque is given by the following expression (Happel & Brenner 1973):

$$\Gamma_z = 8\pi\eta a^2 U_x k^2 g(e), \quad (4.3)$$

with 
$$g(e) = 1.296e + O(e^3) \quad \text{for } e \rightarrow 0. \quad (4.4)$$

Near the axis the sign of  $\Gamma_z$  corresponds to a positive sign of the rotation for the configuration of figure 6. This can be understood physically by stating that the backflow accompanying the motion of the sphere, which is more important in the wider gap symmetric to the off-centring of the sphere, controls the sign of the rotation of the sphere. This argument also suggests a reason for the decrease of the force away from the centre: this situation is more favourable to a decrease in the drag force, as it provides a larger space for the backflow of the liquid in the centre part of the cell.

Results similar to those of Brenner for the force were also obtained using a different method by Hasimoto (1976). The solution of the Stokes equations of motion reduces to a simple boundary-value problem for three harmonic functions.

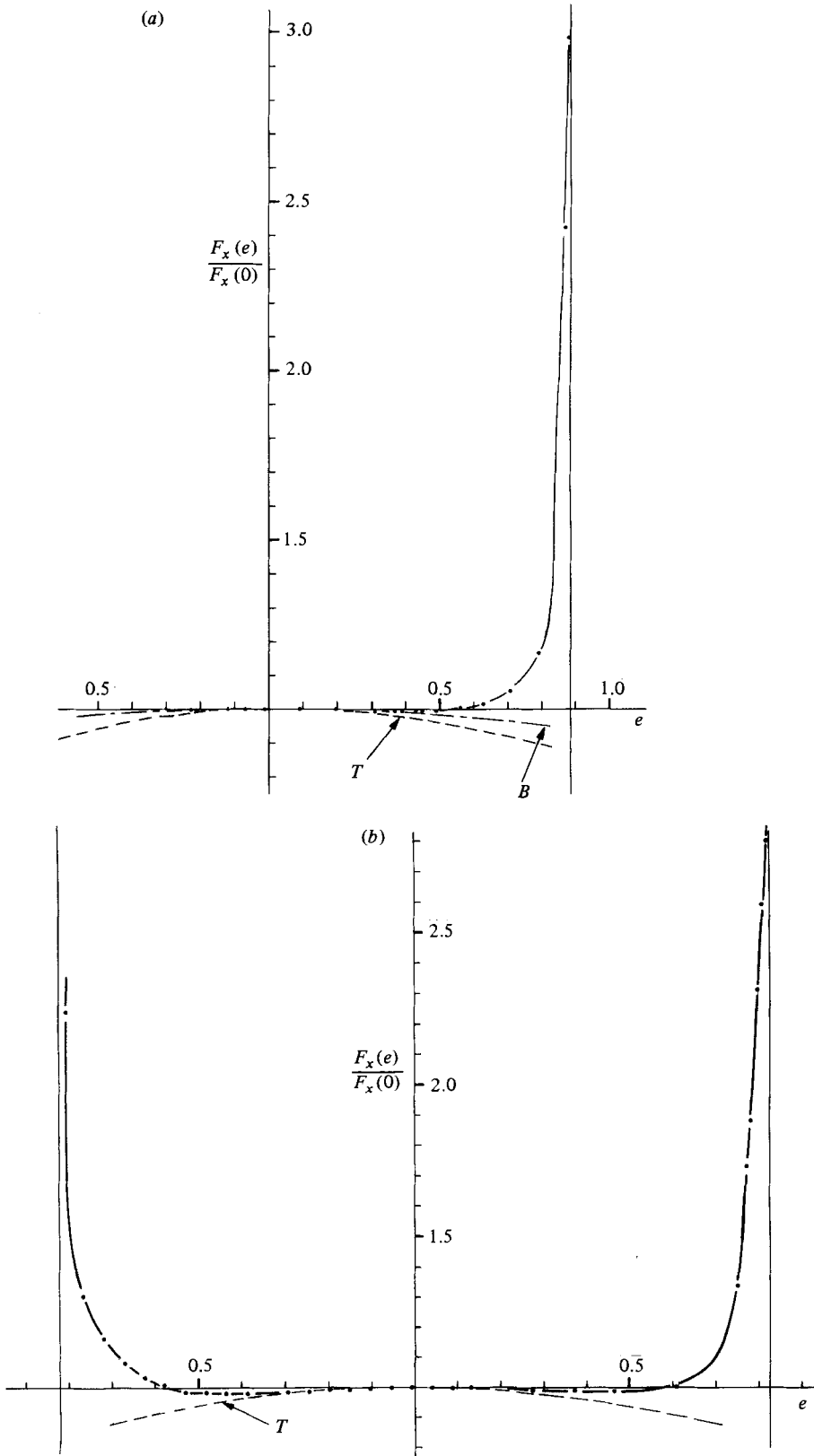


FIGURE 8. For caption see p. 248.

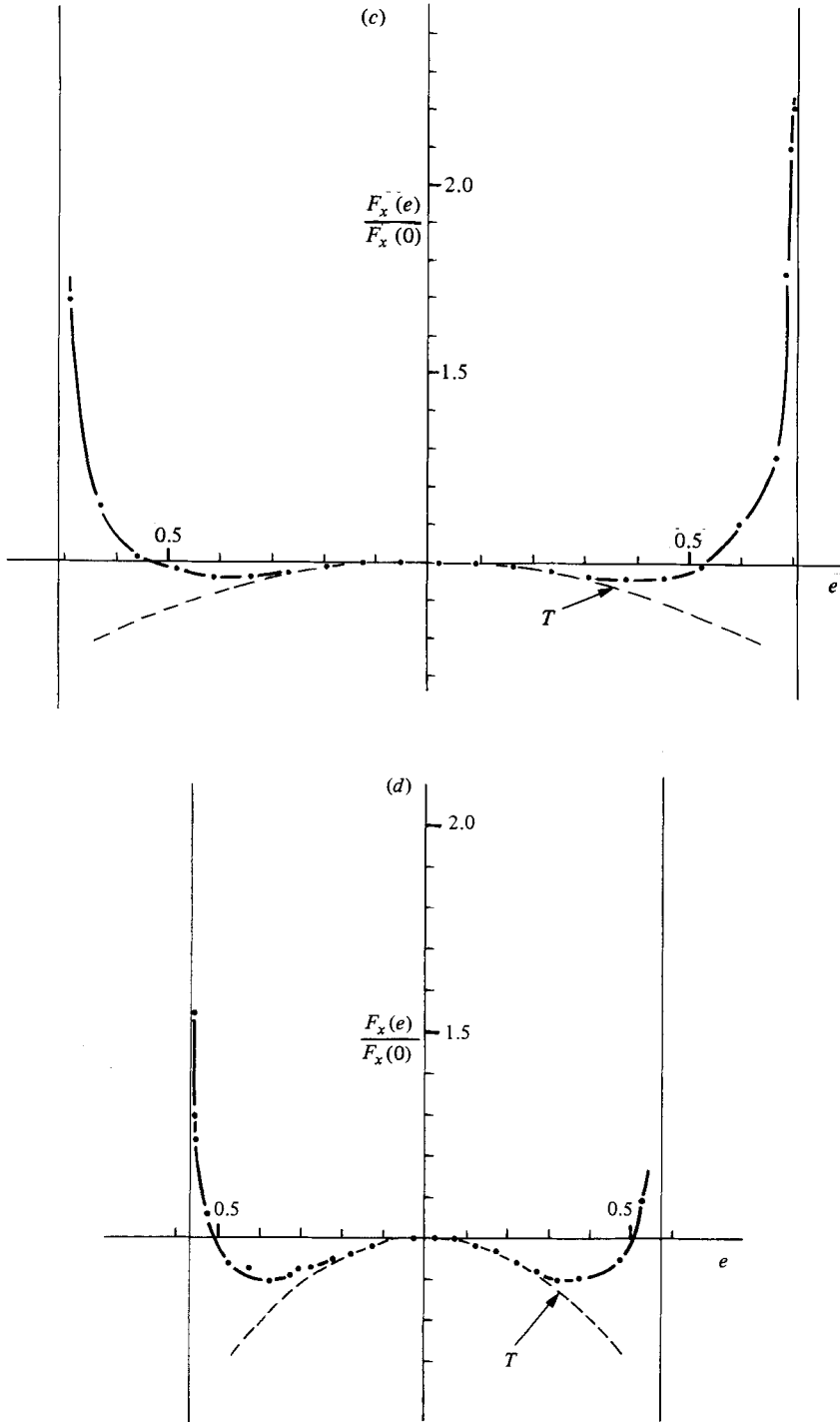


FIGURE 8. For caption see p. 248.

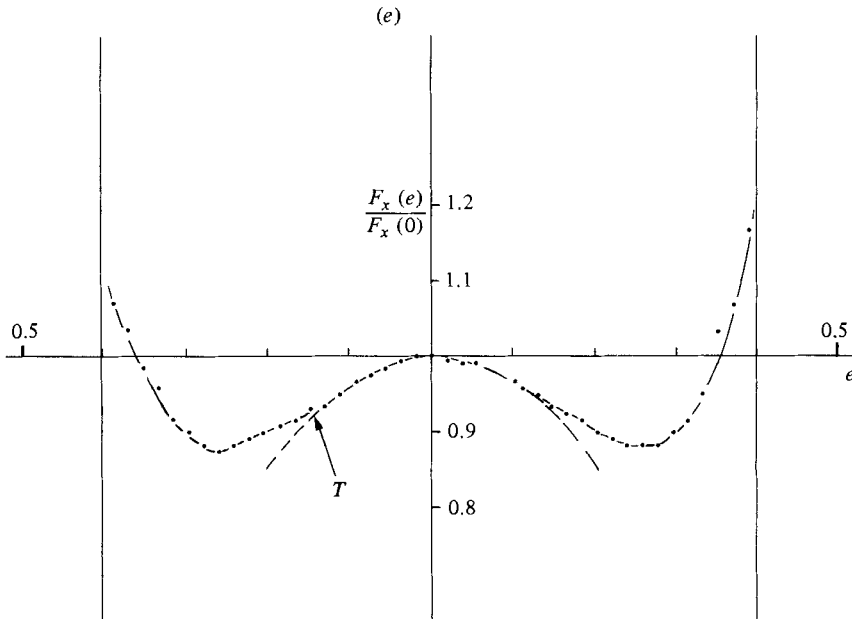


FIGURE 8. The curves in the figure show the variation of the drag force  $F_x(e, k)$  (normalized to its value measured on the axis  $F_x(0, k)$ ) exerted on a sphere moving at the same constant velocity as a function of the eccentricity  $e$  and of the normalized radius  $k$ . ---, the theoretical curves indicated by B and T correspond respectively to Brenner's (1958) and Tözeren's (1983) theories; ..., the experimental points correspond to the following parameters:  $U_x = 6.7 \times 10^{-4} \text{ m s}^{-1}$ ;  $\nu = 10^{-4} \text{ m}^2 \text{ s}^{-1}$  (silicone oil 47V100). (a)  $k = 0.12$  for a sphere of diameter  $2a = 1 \text{ mm}$  and tube of diameter  $2R = 10 \text{ mm}$ ; (b)  $k = 0.17$ ,  $2a = 0.87 \text{ mm}$ ,  $2R = 5 \text{ mm}$ ; (c)  $0.29$ ,  $0.87 \text{ mm}$ ,  $3 \text{ mm}$ ; (d)  $0.44$ ,  $0.87 \text{ mm}$ ,  $2 \text{ mm}$ ; (e)  $0.60$ ,  $0.87 \text{ mm}$ ,  $1.45 \text{ mm}$ .

A more complete analysis was done recently by Tözeren (1983) using a perturbation solution on  $e \ll 1$  but using finite  $k$ -values (up to  $k = 0.7$ ). The results can be summarized using the following expression:

$$F_x(e, k) = 6\pi\eta a U_x [\lambda_0(k) + \lambda_2(k) e^2 + \dots], \quad (4.5)$$

valid for  $e \rightarrow 0$ .

The values  $\lambda_0(k)$  for a sphere falling along the axis of a cylinder given by Tözeren agree with those given by Haberman & Sayre (1958). The values of  $\lambda_2(k)$  are negative, which expresses the decrease of the force away from the axis.

We compare our results with those of Tözeren by calculating the ratio

$$A(e, k) = \frac{F_x(e, k)}{F_x(0, k)} = 1 - \frac{|\lambda_2(k)|}{\lambda_0(k)} e^2 \quad (4.6)$$

and plotting it on figure 8.

The function  $|\lambda_2(k)|/\lambda_0(k)$  (figure 7) increases with  $k$  as found experimentally. Thus we see that our results reproduce quantitatively the variations of (4.1) valid over a large range of  $e$  but for small reduced radii  $k$  and those of (4.5) for small eccentricities  $e$  but for a large range of values of  $k$ ; they also extend these results for arbitrary  $e$  and  $k$ , in particular when the sphere approaches the wall.

To discuss the results in this limit, it is worthwhile to consider the effect of the horizontal component of the force  $F_y$ , which we have neglected by assuming that the position of the sphere was fully determined by the value of the horizontal field.

The horizontal force  $F_y$  induced by inertial effects on a sphere moving with a constant velocity without rotation in a tube has been obtained theoretically by Shinohara & Hasimoto (1979):

$$F_y = \frac{9}{8}\eta a U_x Re h(e); \quad (4.7)$$

$h(e)$  is expressed by infinite series.

The sphere is always found to be pushed towards the axis of the cylinder; the magnitude of  $F_y$  is proportional to  $e$  when  $e$  is sufficiently small, and has a maximum value near the wall. The expression of  $F_y$  is also given by Faxén (1921) in the Oseen approximation and in the limit  $k \rightarrow 0$  (plane wall).

$F_y$  is small in our experimental conditions ( $2a = 0.87$  mm or 1 mm and  $Re \sim 10^{-3}$ ) over most of the range of  $e$ , except possibly in the lubrication regime ( $e \simeq e_{\max}$ ); as the horizontal stability is ensured by the magnetic coils ( $C_1, C_2$ ), we have neglected the effect of  $F_y$ . We have indeed verified from the differential signal between the photodiodes, described in §2.2, that there was no appreciable horizontal displacement of the sphere when the motion was established.

Let us now examine the rotational motion of the sphere. The torque  $\Gamma_z$  experienced by a slightly off-centred sphere can be calculated from (4.3) and (4.4) in the limit  $k \ll 1$ . In the general case where  $k$  is not small, an expansion in powers of  $k$ , valid for  $e \rightarrow 0$ , has been given by Tözere (1983):

$$\Gamma_z = 8\pi\eta a^2 U_x A(k) e + O(e^3). \quad (4.8)$$

$A(k)$  is given by Tözere (1983) (table 2) for  $10^{-3} \leq k \leq 0.7$ .

In all cases, the sphere experiences a positive torque in to the configuration of figure 6. When calculated for the most-unfavourable case (i.e.  $k = 0.6$ ), the hydrodynamic torque is still smaller than that when the sphere is near the lateral wall ( $e \rightarrow e_{\max}$ ). In the latter case, a calculation by Bungay & Brenner (1973) in the conditions  $k \rightarrow 1$  give an asymptotic expression for the torque:

$$\Gamma_z = -\frac{4}{3}\pi\eta a^2 \left(\frac{1-k}{k}\right)^{\frac{1}{2}} U_x \ln \frac{32}{1-e/e_{\max}}. \quad (4.9)$$

In this lubrication limit the torque is negative: it tends to rotate the sphere in the direction of rolling along the lateral wall as in the case of a sphere moving parallel to a plane (Ambari *et al.* 1983).

In the most-unfavourable conditions  $k = 0.6$  and  $e/e_{\max} = 0.99$  with  $2a = 0.87$  mm and  $U_x = 6.7 \times 10^{-4}$  m s $^{-1}$  we get  $\Gamma_z = 2 \times 10^{-8}$  N m, which is 2 orders of magnitude less than the magnetic torque  $\Gamma_m = 2 \times 10^{-6}$  N m (see §2.3). Thus the relative translation of the sphere takes place without any appreciable rotation, because the hydrodynamic torque can be easily compensated by the restoring torque  $\Gamma_m$ .

Let us now consider the variation of the force experienced by the sphere as it gets closer to the sidewalls. On figure 8 we see that the minimum of the force shifts from  $e \sim 0.4$  for  $k = 0.12$  (figure 8*a*) to  $e = 0.25$  for  $k = 0.6$  (figure 8*e*). A similar shift is obtained on the position of intercept of the force curve with the horizontal axis. Beyond this point, the force  $F_x(e, k)$  normalized to  $F_x(0, k)$  increases above unity owing to lubrication. The maximum of the reduced force decreases as  $k$  increases towards 1. This decrease is due to the fast increase of the denominator  $F_x(0, k)$  with  $k$ ; actually,  $F_x(e, k)$  also increases with  $k$  as  $k \rightarrow 1$ . The force  $F_x$  appears to saturate to a finite value as  $e \rightarrow e_{\max}$  (a result already obtained in the case of a plane wall; see figure 10 below). In figure 9, this maximum force has been normalized to  $F_s$ . The normalization has been made using  $\lambda_0(k)$  (see (4.5)), which is known theoretically from the work of Haberman & Sayre (1958) and which we have also measured in independent

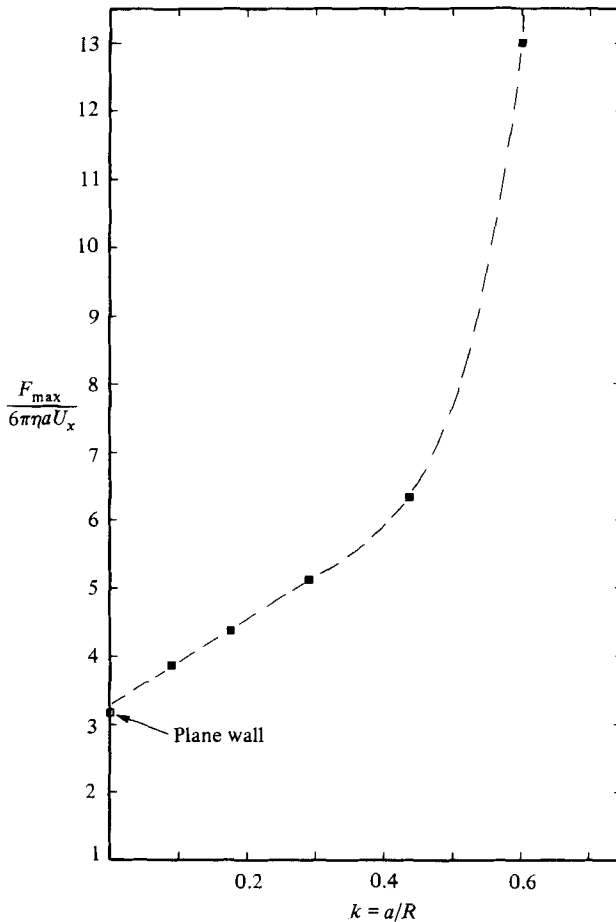


FIGURE 9. The maximum of the drag force  $F_x(e, k)$ , obtained experimentally for  $e \sim e_{\max} = 1 - k$  and normalized to the Stokes force, plotted versus  $k = a/R$  shows the effect of the curvature of the wall in the lubrication limit. The open-square data have been obtained independently by Ambari *et al.* (1983).

experiments. Figure 9 expresses the fact that the curvature of the lateral wall tends to increase the drag on the sphere next to it. We also note that the extrapolation of the ratio  $F(e \sim e_{\max}, k)/F_s$  to  $k = 0$  is very close to that obtained in the case of a sphere moving parallel to a wall. This case has been studied previously by us (Ambari *et al.* 1983), and the results are reproduced on figure 10.

Finally we note that the present results can be compared qualitatively with the observations made by Christopherson & Dowson (1959), by the authors quoted in Bungay & Brenner (1973) and by M. C. Anselmet and R. Blanc (private communication). These observations on a free-falling sphere in a cylindrical tube also show that the sphere gets off-centred from the cylinder axis. It also rotates in a direction opposite to that very near the wall which would correspond to a sphere rolling without sliding against the wall.

We note, however, that the migration away from the axis of the cylinder is in opposite direction from that given by the lateral force  $F_y$  discussed above ((4.7)) due to inertial effects. It is also of a sign opposite to the transverse force  $F_L$  induced by



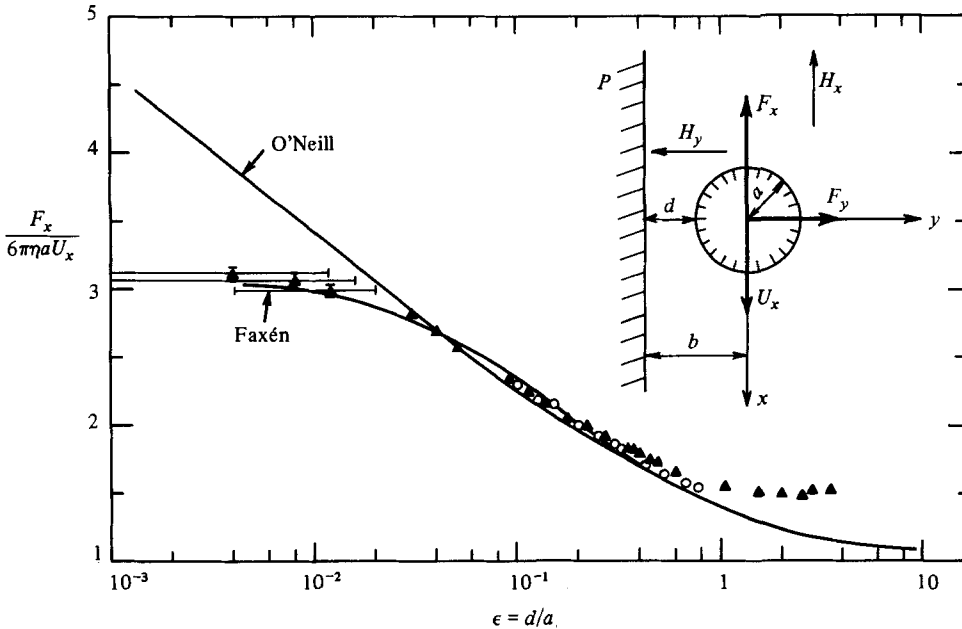


FIGURE 10. The figure gives the value of the vertical force  $F_x$  exerted on a sphere near a wall and normalized to the Stokes force far from it. The distance is measured by the lubrication ratio  $\epsilon = d/a$ . The geometry of the experiment and coordinate system is given schematically ( $\Delta$ , silicone oil 47V100,  $\nu = 10^{-4} \text{ m}^2 \text{ s}^{-1}$ ;  $\circ$ , silicone oil 47V20,  $\nu = 2 \times 10^{-5} \text{ m}^2 \text{ s}^{-1}$ );  $Re \sim 10^{-3}$ . The experimental points depart from the exact solution which O'Neill obtained in the absence of rotation. The saturation effect could be due to the rotation of the sphere when the magnetic torque can no longer balance the hydrodynamic one which diverges as  $e \rightarrow e_{\max}$  (cf. 4.9). The agreement with the approximate solution of Faxén obtained by a reflection method is probably fortuitous.

the spinning of the falling sphere in the positive direction of figure 6. This force was expressed by Rubinow & Keller (1961) as

$$F_L = \pi a^3 \rho \boldsymbol{\Omega} \times \mathbf{U}_x [1 + O(Re)], \quad (4.10)$$

where  $\boldsymbol{\Omega}$  is the angular velocity;  $F_L$  is directed towards the axis.

The physical explanation of the migration force has its origin in the backflow induced by the motion of the sphere, which is limited by the lateral walls of the cylinder tube. The backflow was observed in the reference frame of the cylinder as a vortex ring around the sphere by Coutanceau (1968) (figure 3–5). This vortex gets asymmetric when the sphere moves sideways in such a way as to minimize viscous dissipation in this low-Reynolds-number case. The motion of the sphere away from the centre in the experiments under an imposed force field must have the same origin as the decrease of the vertical force we have observed in our experiments.

## 5. Conclusion

The present experimental work has made use of an original viscometer using a sphere moving at a fixed velocity relative to a liquid and measuring the force exerted on the sphere. We have studied two types of interaction of a sphere with a solid surface. In the unsteady problem of a sphere moving towards a plane wall, we have

found an increase of the Stokes force due to lubrication effects, in agreement with theoretical models formulated for this problem. An interesting extension, not possible with conventional experiments where the force on a sphere is imposed, would be to study time-dependent (Basset-integral) inertial effects; this is a realizable extension of the present work. The second experiments deal with the stationary motion of a sphere parallel to the axis of a cylindrical tube. The results confirm theoretical findings which show a decrease of the Stokes force away from the centre of the tube, the existence of a minimum and a further increase when the sphere approaches the sidewalls. In this limit they also show the effect of the wall curvature with respect to the motion parallel to a flat wall. In this geometry our results extend the range of variation of the variables of the theories. In our experiment the rotation of the sphere was negligible, but one should be able to measure the torque exerted on the magnetic sphere if it were larger.

The experiments are of direct relevance to practical problems of motion of suspended solid objects in limited geometries. They also illustrate some of the basic problems in the hydrodynamics of suspensions: the lubrication effects which control the relative approach of spheres in shear flows, or the backflow effect which causes the decrease of the sedimentation velocity of a finite concentration of spheres. More direct applications of the present apparatus to the hydrodynamics of suspensions can be designed easily: unsteady motion of a sphere parallel to or towards another spherical object; drag force on a particular sphere sedimenting in a fixed bed (the magnetic sphere having its position controlled magnetically while the other spheres are held fixed mechanically with very thin threads), or in a bed of freely sedimenting particles around the control sphere. Another possibility (indicated by a referee) is to study the approach of a sphere to a horizontal free surface or interface (see Lee, Chadwick & Leal 1979; Lee & Leal 1980; O'Neal & Ranger 1983). We had indeed tried such an experiment, but there are difficulties due to the deformation of the surface as the sphere approaches it, which is controlled by the crista effect. It is the hope of the authors that the present work will stimulate interactions with the community of fluid-mechanicians studying heterogeneous matter to define crucial projects around a very versatile tool of experimentation.

One of us (B.G.-M.) acknowledges a grant from C.E.A. (Laboratoire L. Brillouin) for the time during which this research was performed. The authors wish to thank Professor de Gennes, who introduced us to suspension problems. We wish also to thank M. Clement for his generous assistance and D. Lhuillier, J. F. Brady, Y. Pomeau and F. Feuillebois for helpful discussions.

#### REFERENCES

- AMBARI, A., GAUTHIER-MANUEL, B. & GUYON, E. 1983 Effect of a plane wall on a sphere moving parallel to it. *J. Phys. Lettres* **44**, L143-L146.
- BATCHELOR, G. K. 1972 Sedimentation in a dilute dispersion of spheres. *J. Fluid Mech.* **52**, 245-268.
- BRENNER, H. 1961 The slow motion of a sphere through a viscous fluid towards a plane surface. *Chem. Engng Sci.* **16**, 242-251.
- BRENNER, H. & HAPPEL, J. 1958 Slow viscous flow past a sphere in a cylindrical tube. *J. Fluid Mech.* **4**, 195-213.
- BUNGAY, P. M. & BRENNER, H. 1973 The motion of a closely-fitting sphere in a fluid-filled tube. *Intl J. Multiphase Flow* **1**, 25-56.

- CHRISTOPHERSON, D. G. & DOWSON, D. 1959 An example of minimum energy dissipation in viscous flow. *Proc. R. Soc. Lond. A* **251**, 550–564.
- COOLEY, M. D. A. & O'NEILL, M. E. 1969 On the slow motion generated in a viscous fluid by the approach of a sphere to a plane wall or stationary sphere. *Mathematika* **16**, 37–49. (Note that in their calculations a factor of  $\frac{1}{2}$  has been omitted.)
- COUTANCEAU, M. 1968 Mouvement uniforme d'une sphère dans l'axe d'un cylindre contenant un liquide visqueux. *J. Méc.* **7**, 49–67.
- COX, R. G. & BRENNER, H. 1967 The slow motion of a sphere through a viscous fluid towards a plane surface – II. Small gap widths including inertial effects. *Chem. Engng Sci.* **22**, 1753–1777.
- DE GENNES, P. G. 1981 Dynamics of concentrated dispersions: a list of problems. *Physico-Chem. Hydrodyn.* **2**, 31–44.
- FAMULORO, J. 1962 D.Eng.Sci. thesis. New York University.
- FAXÉN, H. 1921 Einwirkung der Gefäßwände auf den Widerstand gegen die Bewegung einer kleinen Kugel in einer zähen Flüssigkeit. Diss. Uppsala, pp. 55–128.
- GAUTHIER-MANUEL, B. & GUYON, E. 1980 *C.R. Acad. Sci. Paris B* **290**, 465–467.
- GAUTHIER-MANUEL, B., MEYER, R. & PIERANSKI, P. 1984 *J. Phys. E: Sci. Instrum.* (to appear).
- GOLDMAN, A. J., COX, R. G. & BRENNER, H. 1967 Slow viscous motion of a sphere parallel to a plane wall – I. Motion through a quiescent fluid. *Chem. Engng Sci.* **22**, 637–651.
- HABERMAN, W. & SAYRE, R. M. 1958 *David Taylor Model Basin Rep.* 1143 (US Navy Dept, Washington DC).
- HAPPEL, J. & BRENNER, H. 1973 *Low Reynolds Number Hydrodynamics*. Noordhoff.
- HASIMOTO, H. 1976 Slow motion of a sphere in a cylindrical domain. *J. Phys. Soc. Japan, Lett.* **41**, 2143–2144.
- LEE, S. H., CHADWICK, R. S. & LEAL, L. G. 1979 Motion of a sphere in the presence of a plane interface. Part 1. An approximate solution by generalization of the method of Lorentz. *J. Fluid Mech.* **93**, 705–726 (and Corrigendum, *J. Fluid Mech.* **104** (1981) 534).
- LEE, S. H. & LEAL, L. G. 1980 Motion of a sphere in the presence of a plane interface. Part 2. An exact solution in bipolar co-ordinates. *J. Fluid Mech.* **98**, 193–224.
- LORENTZ, H. A. 1907 *Abhandl. theor. Phys. (Leipzig)* **1**, 23.
- MACKAY, G. D. M. & MASON, S. G. 1961 Approach of a solid sphere to a rigid plane interface. *J. Colloid Sci.* **16**, 632–635.
- MACKAY, G. D. M., SUZUKI, M. & MASON, S. G. 1963 Approach of a solid sphere to a rigid plane interface – Part 2. *J. Colloid Sci.* **18**, 103–104.
- MAUDE, A. D. 1961 End effects in a falling sphere viscometer. *Brit. J. Appl. Phys.* **12**, 293–295.
- O'NEILL, M. E. 1964 A slow motion of viscous liquid caused by a slowly moving solid sphere. *Mathematika* **121**, 67–74.
- O'NEILL, M. E. & RANGER, K. B. 1983 The approach of a sphere to an interface. *Phys. Fluids* **26**, 2035–2042.
- O'NEILL, M. F. & STEWARTSON, K. 1967 On the slow motion of a sphere parallel to a nearby plane wall. *J. Fluid Mech.* **27**, 705–724.
- RUBINOW, S. I. & KELLER, J. B. 1961 The transverse force on a spinning sphere moving in a viscous fluid. *J. Fluid Mech.* **11**, 447–459.
- SHINOHARA, M. & HASIMOTO, H. 1979 The lateral force on a small sphere sedimenting in a viscous fluid bounded by a cylindrical wall. *J. Phys. Soc. Japan* **46**, 320–327.
- STIMSON, M. & JEFFERY, G. B. 1926 The motion of two spheres in viscous fluid. *Proc. R. Soc. Lond. A* **111**, 110–116.
- TÖZEREN, H. 1983 Drag on eccentrically positioned spheres translating and rotating in tubes. *J. Fluid Mech.* **129**, 77–90.
- YUU, S. & FUKUI, Y. 1981 Measurement of fluid resistance correction factor for a sphere moving through a viscous fluid toward a plane surface. *AIChE J.* **27**, 168–170.